PLASMA HEATING AND LOSSES IN TOROIDAL MULTIPOLE FIELDS

C. J. Armentrout, J. D. Barter, R. A. Breun, A. J. Cavallo,
J. R. Drake, J. F. Etzweiler, J. R. Greenwood, W.C. Guss,
D. W. Kerst, G. A. Navratil, R. S. Post, J. W. Rudmin,
G. L. Schmidt, J. C. Sprott, and K. L. Wong

September 1974

(Presented at Tokyo IAEA Conference, November 1974)

PLP 606

Plasma Studies

University of Wisconsin

COO-2387-34

PLASMA HEATING AND LOSSES IN TOROIDAL MULTIPOLE FIELDS

C. J. Armentrout, J. D. Barter, R. A. Breun, A. J. Cavallo,
J. R. Drake, J. F. Etzweiler, J. R. Greenwood, W. C. Guss,
D. W. Kerst, G. A. Navratil, R. S. Post, J. W. Rudmin,
G. L. Schmidt, J. C. Sprott, and K. L. Wong

September 1974

Plasma Studies
University of Wisconsin

PLASMA HEATING AND LOSSES IN TOROIDAL MULTIPOLE FIELDS*

C. J. Armentrout, J. D. Barter, R. A. Breun, A. J. Cavallo, J. R. Drake, J. F. Etzweiler, J. R. Greenwood, W. C. Guss, D. W. Kerst, G. A. Navratil, R. S. Post, J. W. Rudmin, G. L. Schmidt, J. C. Sprott, and K. L. Wong

University of Wisconsin, Madison, Wisconsin USA

ABSTRACT

The heating and loss of plasmas have been studied in three pulsed, toroidal multipole devices: a large levitated octupole, a small supported octupole and a very small supported quadrupole. Plasmas are produced by gun injection and heated by electron and ion cyclotron resonance heating and ohmic heating. Electron cyclotron heating rates have been measured over a wide range of parameters, and the results are in quantitative agreement with stochastic heating theory. Electron cyclotron resonance heating produces ions with energies larger than predicted by theory. With the addition of a toroidal field, ohmic heating gives densities as high as $10^{13}cm^{-3}$ in the toroidal quadrupole and $10^{12}cm^{-3}$ in the small octupole.

Plasma losses for $n = 5 \times 10^{9}cm^{-3}$ plasmas are inferred from Langmuir probe and Fabry-Perot interferometer measurements, and measured with special striped collectors on the wall and rings. The loss to a levitated ring is measured using a modulated light beam telemeter. The confinement is better than Bohm but considerably worse than classical. Low frequency convective cells which are fixed in space are observed. These cells around the ring are diminished when a weak toroidal field is added, and loss collectors show a vastly reduced flux to the rings. Analysis of the spatial density profile shows features of B-independent diffusion. The confinement is sensitive to some kinds of dc field errors, but surprisingly insensitive to perturbations of the ac confining field.

*This work was supported by the U. S. Atomic Energy Commission.

I. PLASMA HEATING

Electron Cyclotron Resonance Heating: ECRH has been a standard means of producing and heating plasmas in toroidal multipoles. Recent experiments on the small octupole have permitted quantitative measurements of electron heating rates over a wide range of parameters. These studies have used a relatively low power ($\lesssim$ 100 watts) microwave source to sweep through an isolated cavity mode or to excite a number of adjacent modes whose Q can be measured. The perturbation in Q due to the presence of the plasma gives a measure of the heating rate. Fig. 1 shows the heating rate as a function of resonance zone position which is specified by the ratio of the resonance zone magnetic field to the maximum magnetic field in the octupole. G is the normalized heating rate which is proportional to the average power absorbed per electron. G can be calculated from single particle heating theory and it is in reasonably good agreement with the experimental results at low electron densities. At high electron densities, the penetration problem can reduce the heating rate if the microwaves are not launched on a magnetic beach. Fig. 2 shows the heating rate as a function of electron density with resonance zones near the rings of the octupole. The accessibility problem accounts for the fall off of the heating rate at high densities. When the resonance zone is near the center of the octupole, no such fall off is observed. The neutral density, electric field strength and electron plasma temperature are varied, and the heating rate is not sensitive to the variation of these parameters at low plasma densities as expected from the single particle heating theory.

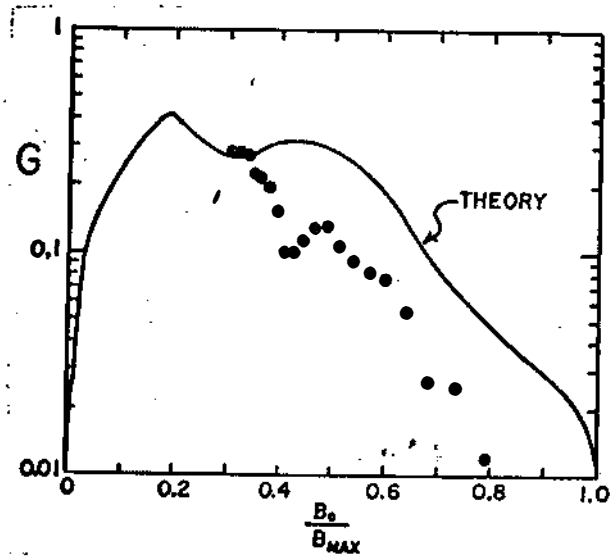

Fig. 1. ECRH rate vs position of resonance zone

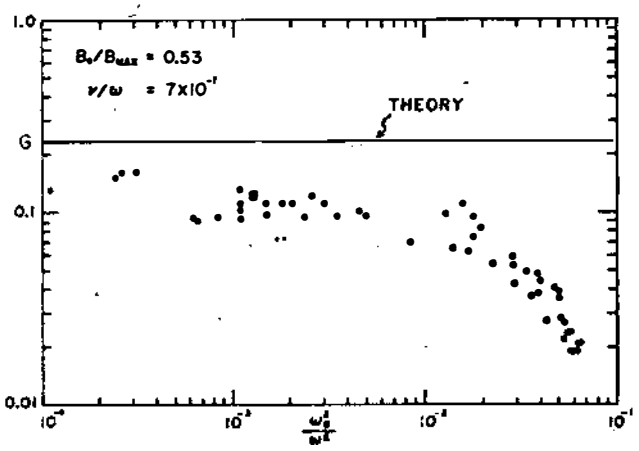

Fig. 2. ECRH rate vs electron density

A short (200 μsec), high power (100 kW), pulse of microwaves at the electron cyclotron frequency produce an anisotropic component of energetic electrons ($\lesssim$ 10 (keV) which have a long lifetime ($\lesssim$ 10 msec) in the levitated octupole. Since maximum heating occurs off the separatrix, the long lifetime electrons occur

only with high initial density ($\sim 10^{10} cm^{-3}$) and high neutral pressure ($> 10^{-6}$ Torr H_2), so they do not dominate the pressure profile. Also a slight B_T ($B_p/B_T \sim 3$ at resonance zone) and full levitation are necessary. The latter condition could be superficial. The electrons mirror in the low field side of the ring opposite both the detector and the supports. Since the electrons must sustain a collision to be detected, the ring supports could just be interrupting the electrons driving the detection signal into the noise level.

For a shorter microwave pulse ($\lesssim 30$ μsec) into a low initial density ($\sim 5 \times 10^{8} cm^{-3}$) and low neutral pressure ($\sim 5 \times 10^{-7}$ Torr), the hot electrons dominate the pressure profile. Various large potential oscillations are observed and ions are heated as well as electrons. Average ion energy rises about 15 eV. The distribution is non-Maxwellian with 1 keV energy ions observed.

Capacative probes observe oscillations (ω_1) which are $\sim \omega_{pi} \gtrsim 2\,\omega_{ci}$ and have an amplitude of 50 volts peak-to-peak. Also a very low frequency (ω_2) floating potential difference of up to 200 volts along field lines is observed. For ω_1 to be identified as a decay instability product from the incident microwaves a third wave (ω_3) must be observed where $\omega_3 = \omega_{\mu wave} - \omega_1$. With an unshielded probe tip, no high frequency wave (ω_3) was observed to within 5 orders of magnitude of the incident microwave signal. With a screened tip no purely electrostatic wave at ω_3 was observed either. Oscillations in the range of the electron plasma frequency (240 MHz $< \omega_3/2\pi <$ 1800 MHz) were observed, however.

Ion Cyclotron Resonance Heating: RF electric fields at the ion cyclotron frequency ($\sim$ 1 MHz) are produced by an electrostatically shielded fifth ring coaxial to the four main rings and located near the wall. The inductive electric field easily penetrates the plasma at densities up to $3 \times 10^{12} cm^{-3}$. A 100 kW oscillator provides a 144 μsec pulse of 1 MHz rf, raising the ion temperature from $\lesssim$ 3 eV to $\sim$ 30 eV as measured by an electrostatic analyzer. The fifth ring in parallel with resonating capacitors forms the tank circuit of the oscillator. The resistive loading of the fifth ring by the plasma is measured by a null technique. The voltage applied to the fifth ring and the drive current of the tank are compared, the difference from a null condition being experimentally calibrated. The particle heating measured with the energy analyzer and the power supplied to the plasma as inferred from the loading measurements are compared to stochastic heating theory in Fig. 3. A higher power (500 kW) oscillator with improved impedance match to the plasma and improved coupling structure are being developed.

Ohmic Heating: The primary ohmic heating experiment in the small supported toroidal quadrupole ($2 \times 10^{4} cm^{3}$). The time changing poloidal confinement field ($\tau_{1/2} = 1.2$ msec) is coupled with either a crowbarred or falling toroidal field ($\tau_{1/2} = .6$ msec). In the latter case for peak poloidal and toroidal fields of 10 and 3.5 kG a maximum $\langle E_{||} \rangle$ of 200 mV/cm is sustained for 300 μsec. Because of the radial dependence of a quadrupole field near its magnetic axis, plasma currents generated

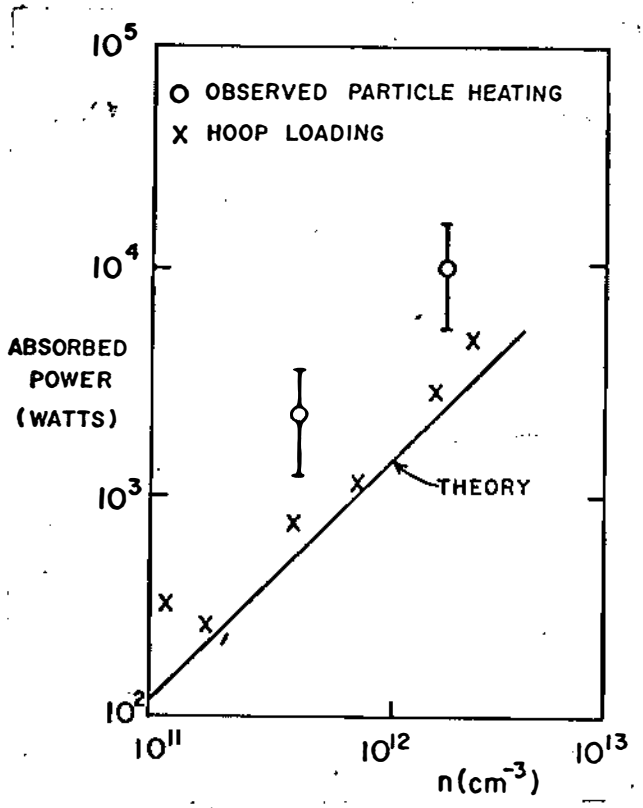

Fig. 3. ICRH power absorbed by the plasma vs electron density.

radiation (CI-CIV) then represents a major loss. kT_e remains in the 10 eV range. The spatial distribution of the profile is shown in Fig. 4.

Similar experiments are under way on the small octupole, using the electric field induced by the rise and decay of the toroidal field, or the decay of the octupole field, starting with a microwave-produced plasma. An on-axis toroidal current density of 4.4 A/cm^2 was observed for an applied toroidal magnetic field of 1.3 kG and half period 1.8 msec, giving a q of 11. For the same octupole field and H_2 filling pressure, application of a faster pulsed (half period 1.0 msec) toroidal field of the same magnitude resulted in a plasma with

(10kA) are not sufficient to alter the basic vacuum field structure. Toroidal and poloidal current components have decay times of ~ 100 μsec determined by the time changing rotational transform and $\langle E_{||} \rangle$. Local conductivity for the bulk of the plasma is consistent with Spitzer (10 eV) except outside the current peak where large, low frequency fluctuations exist. A broad spectrum of density fluctuations (20-200 kHz) is observed in the region of inverted pressure gradient outside the density peak where electron drift and thermal speeds are comparable. High frequency fluctuations (1 MHz) are present near the ring. Densities $> 10^{13}$cm^{-3} are produced with increased input power but carbon

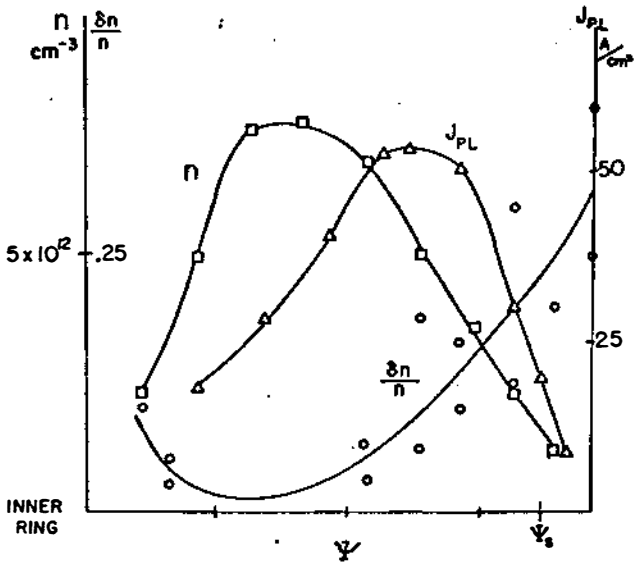

Fig. 4. Spatial distribution of plasma current (J_{pl}), density (n), and density fluctuations ($\delta n/n$) near the inner ring of the toroidal quadrupole.

toroidal current density of 1.2 A/cm^2 on axis, corresponding to q = 40, total
3.5 cm, and n_e on axis of 2×10^{11}cm^{-3}. Surrounding this plasma is a ring of denser plasma $n_e \tilde{=} 6\times10^{11}$cm^{-3}, created by a poloidal ohmic heating current induced by the rise of the toroidal field.

II. PLASMA LOSSES

Fluctuations: The low frequency (10-20 kHz) fluctuation spectrum in the levitated octupole has been examined using correlation routines written for the computer data acquisition system developed here. The waves have been examined for gun injected plasmas ($n\tilde{}5\times10^9$cm^{-3}) with the poloidal B field only. The results are similar for the fluctuation spectrum seen both at peak field and in the early, rising B portion of the pulse. The frequency is quite sensitive to the presence of obstacles such as supports and probes nearby in the plasma. High impedance double probes located 1 cm apart along a B line are in phase to within 0.1% of the fluctuation period, indicating $\nabla_{||}$ Potential = 0 and $\lambda_{||}$ is longer than the (closed) field line. The toroidal phase velocity of the waves has been measured with pairs of probes separated toroidally. The rotational angular frequency is typically $2\text{-}3\times10^3$sec^{-1} in the ion diamagnetic drift direction and is a function of ψ. The phase velocity is typically 3×10^5cm/sec with a 20 cm wavelength. Density gradients give the value of the diamagnetic
$\vec{E} \times \vec{B}$ velocity which is found to be equal to and parallel with the diamagnetic velocity. The sum of these measured values is within 10% of the measured toroidal wave velocity. These observations indicate that plasma potentials and the associated density gradients drive the toroidal motion of the waves and the background plasma. The fluctuation level $\delta N_{rms}/N$ rises from a fraction of a percent at the separatrix to its maximum value at ψ_{crit} of typically 25% and it drops only slightly outward to the wall. This fluctuation decreases with increasing field strength. At the wall, δ N is independent of B but drops 40% at ψ_{crit} with a 60% increase in B.

The correlation coefficient between δ N at the wall seen by a stripped collector and the δ N seen by a movable probe drops from (typically) 80% just outside ψ_{crit} to 10% at ψ_{sep}. This crossfield correlation coefficient of the waves at ψ_{crit} drops by 1/3 with a 60% increase in B. The crossfield phase velocity is outwards, essentially independent of B.

Convection Cells: Closed floating potential contours or cells ($\delta\phi=0.3\ kT_e/e$) are observed in the private flux region of a ring for plasmas with $n\tilde{}5\times10^9$cm^{-3} and $\omega_{pi}\tilde{}\omega_{ci}$. The $\vec{E} \times \vec{B}$ circulation times are several milliseconds. The cell structure is reproducible, suggesting that the cells are generated by some permanent structural feature of the machine such as the poloidal gap or some inherent field error. Since the hoop surface is an equipotential, $\vec{E} \times \vec{B}$ drifts cannot carry the plasma all the way to the hoop, although the observed electric fields in the body of the plasma can cause crossfield fluxes of the

order of 1% to 10% of Bohm. These cells are diminished with full levitation when a weak toroidal field (B_T=0.1 B_p at the surface of the outer ring) is added. The observed cells might bear a relation to long wave vortices predicted by guiding center theory.[1]

Floating potential contours over a 90° azimuthal segment of the private flux region near the gap for the case of a purely poloidal field and the case with the toroidal field are shown in Fig. 5. The hoops were fully levitated for both cases. When the toroidal field was added, the cell structure was smoothed and the potential contours became azimuthally symmetric.

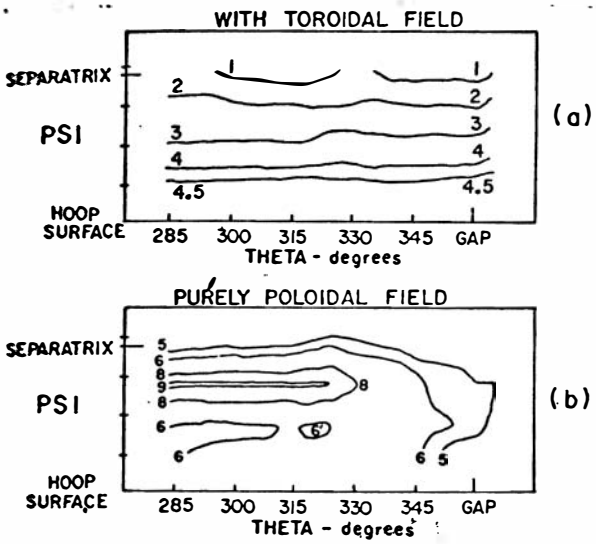

Fig. 5. Contours of equal floating potential (volts) in the private flux region in the vicinity of the insulated poloidal field gap.

The high density plasma has $\omega_{pi} \sim 10\ \omega_{ci}$ and, for a purely poloidal field, examination of a quarter sector of the toroid showed a lack of cell structure described above.

Surface Plasma Flux: The region around an internal ring in an octupole can have absolute MHD stability when the plasma density gradient is directed away from the ring. For this reason the details of plasma transport and behavior near such a ring are of special interest. Plasma losses to an outer ring were measured by the striped surface collectors developed at the University of Wisconsin.

Adding a weak toroidal field to the octupole ($B_T \approx 0.1\ B_p$ at the surface of the outer ring) reduced particle loss to a fully levitated ring by about a factor of 10 for a hot ion ($kT_i \approx 20$-40 eV, $kT_e \approx 5$ eV) plasma. Losses had to be measured via a telemeter, with all wires, probes, and supports removed from the vicinity of the ring since such obstacles alter the natural loss. Under these circumstances, a large burst of plasma loss near injection is followed by a quiet period, then, under some circumstances, by a burst of noise on the collector current, and then a further quiet period. It was found that even a 0.75 mm diameter wire obstacle 6 mm from the ring but

[1] For a discussion of vortices associated with guiding-center theory see: J. B. Taylor and B. McNamara, Phys. Fluids 14, 1492 (1971) and H. Okuda and J. M. Dawson, Phys. Fluids 16, 408 (1973) and G. Joyce and D. Montgomery, Journ. of Plasma Physics 10, 107 (1973).

60° away from a collector around the major circumference of the ring drastically affected collector current. This obstacle eliminated the burst of noise on the collector current and somewhat reduced the magnitude of the current at all times. Evidently, probe measurements made near a fully levitated ring must be interpreted with great care since the probe itself is an obstacle.

Floating potential profiles were taken near the ring with a high impedance Langmuir probe. For the poloidal field only case, the profile was quite flat, and the ring floating potential was quite close to the floating potential of the main body of the plasma. With the added toroidal field, the floating potential profile was similar to that of the poloidal field only case, but the ring itself floated to a much higher positive voltage ($\geq$+10V). Evidently, the added toroidal field strongly inhibited electron transport to the ring with the hot ion plasma. Using a ring itself as an electrode give an ambiguous result since the measured loss changes as the collecting potential is raised.

A local crossfield diffusion coefficient was defined as follows:

$$D\left(\frac{cm^2}{sec}\right) = \frac{\text{Particle flux to collector}}{\text{Density gradient near the ring}}$$

This was determined for different magnetic field strengths with and without the added toroidal field. Loss to the ring was measured via telemeter, with all obstacles removed from the vicinity of the ring. The density gradient near the ring was measured with a Langmuir probe, and it was assumed that this did not change when the probe was removed from the region next to the ring. The results of these measurements and calculations are shown in Table I.

Thus, from direct measurement of particle loss to a ring via a telemeter and observations of the floating voltage of a support free ring, we conclude that confinement properties in octupoles are different with and without a toroidal field. When such a field is added, a shearless layer is formed near the wall and within the last MHD stable flux surface. This layer is highly sensitive to field perturbations. Striped collectors on some sections of the octupole wall have measured large increases in plasma loss with the added toroidal field.

Field Errors: Various types of magnetic field perturbations were applied and the floating potential in the vicinity of the perturbations was scanned. Field errors which left poloidal field lines inside ψ_{crit} closed did not generate any observable structure. Relatively large field errors can leave field lines closed if certain symmetry and perturbation orientation conditions are satisfied.[2] On the other hand,

[2] J. R. Drake, in the Proceedings of the 1st International IEEE Conference on Plasma Science, Knoxville, Tennessee (1974).

errors which drew field lines from the containment zone out through the conducting vacuum tank wall (dc field errors) or errors which drew field lines through the obstacle-like perturbation (field errors pulsed with the same time dependence as the main field and located between ψ_{crit} and the vacuum tank wall) could generate structure in the plasma. When the field error was applied to a plasma ($n \approx 5 \times 10^9 cm^{-3}$) with no ring supports present a positive center cell was generated. Similar positive-center cells were generated by ring support obstacles. When both the field error and the supports were present both positive-center and negative-center cells appeared. Examples of the cell structure generated by a dc perturbation and ring support obstacles are shown in Fig. 6.

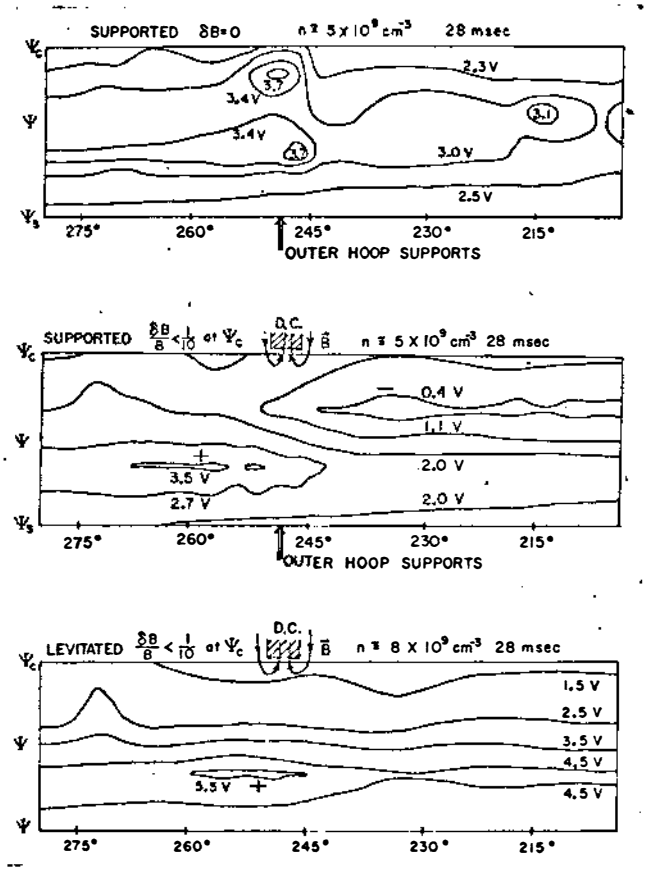

Fig. 6. Convection cells generated by a dc field error.

The field errors applied to the toroidal quadrupole are always dc because of the stainless steel vacuum vessel. At four azimuthal locations, pairs of dipoles, above and below the vacuum vessel, produced a 4% perturbation in the poloidal field. The plasma density was $10^{10} cm^{-3}$ and $kT_e = 1$ eV. For parallel moments, large losses to the walls and rings resulted with a distribution consistent with plasma streaming along field lines leaving the confinement region. Antiparallel dipoles produced no change in the losses over the unperturbed plasma.

Behavior at High Densities: A longer version of the coaxial plasma gun has been constructed giving a higher efficiency of plasma production. About 60% of the neutral gas initially injected is expelled as plasma from the gun. The gun has been placed directly on the side of the large octupole resulting in peak densities of $\sim 2 \times 10^{12} cm^{-3}$ and trapping efficiencies of $\sim$ 80% with very good reproducibility (< 5% shot-to-shot density variation).

At this density the initial ion temperature is $\sim$ 10 eV. The ions rapidly cool ($\sim$ 200 μsec) to 1 eV due to charge exchange with the neutral gas accompanying injection. The electron temperature cools to 1.5 eV in 4 msec and remains constant for the duration of the experiment. At these

temperatures, densities, and neutral densities the plasma is dominated by Coulomb interactions with λ_{ei}~10 cm. Profile evolution (see Fig. 7) is toward a rather flat profile. Large fluctuations are observed, localized in the bad curvature region (ballooning mode) propagating perpendicular to $\vec{B}$. The fluctuations extend from well inside ψ_s out to ψ_c with largest amplitude occuring midway between ψ_c and ψ_s. At that point $\frac{\delta n}{n}$ = 0.4-0.5 with $\delta\emptyset$ ~ 0.3 volts, $\omega=10^4$-$10^5 sec^{-1}$, and $K_{||}$~1 cm^{-1}. ω increases roughly linearly with B and $K_{||}$ decreases with increasing B. diffusion coefficient

$D = \frac{K}{B}\langle \delta n_i \delta\emptyset \rangle / \nabla n \sim 1\ m^2 sec^{-1}$

is roughly equal to the Bohm value and agrees with the observed plasma lifetime of ~5 msec.

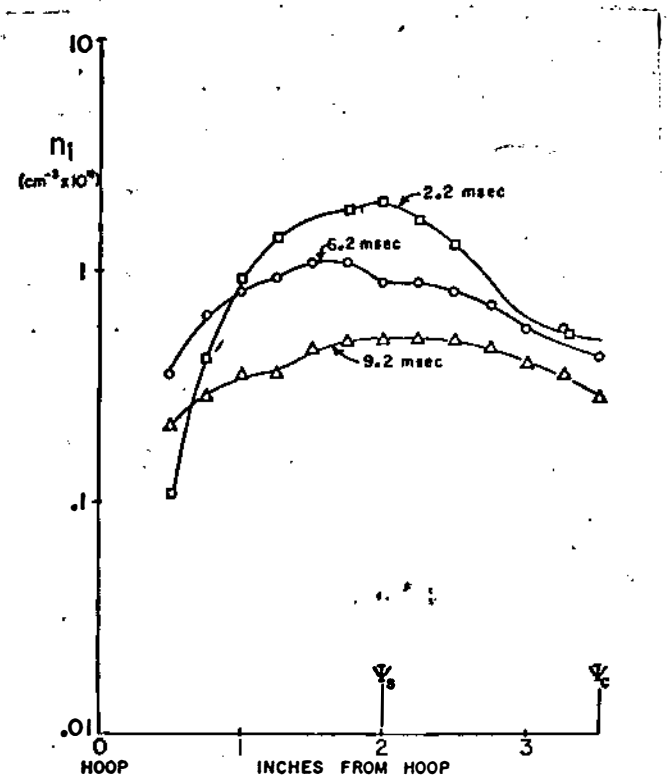

Fig. 7 Evolution of profile for a high density plasma in the levitated octupole.

Table I. Diffusion Coefficient (D) vs Magnetic Field (B)

	1.2 kG	1.8 kG	2.4 kG	3.0 kG
B Poloidal only D $\left(\frac{cm^2}{sec}\right)$	800	620	780	765
B Poloidal and Toroidal	63	62	55	48
Bohm Diffusion				10,000

Figure Captions

1. ECRH rate vs position of resonance zone.
2. ECRH rate vs electron density.
3. ICRH power absorbed by the plasma vs electron density.
4. Spatial distribution of plasma current (J_{pl}), density (n), and density fluctuations ($\delta n/n$) near the inner ring of the toroidal quadrupole.
5. Contours of equal floating potential (volts) in the private flux region in the vicinity of the insulated poloidal field gap.
6. Convection cell generated by a dc field error.
7. Evolution of profile for a high density plasma in the levitated octupole.